

EXPERIMENTAL RESEARCH INTO DYNAMIC PROPERTIES OF MASONRY BARREL VAULTS NON-REINFORCED AND REINFORCED WITH CARBON COMPOSITE STRIPS

Zigler Radek¹, Witzany Jiří¹, Makovička Daniel², Urushadze Shota³,
Pospíšil Stanislav³, Kubát Jan¹, and Kroftová Klára⁴

1. CTU in Prague, Faculty of Civil Engineering, Department of Building Structures, Prague, Thákurova 7, Czech Republic; zigler@fsv.cvut.cz, witzany@fsv.cvut.cz, jan.kubat.2@fsv.cvut.cz
2. CTU in Prague, Klokner Institute, Prague, Šolínova 7, Czech Republic; daniel.makovicka@klok.cvut.cz
3. The Institute of Theoretical and Applied Mechanics AS CR, v. v. i, Prague, Prosecká 809/76, Czech Republic; urushadze@itam.cas.cz, pospisil@itam.cas.cz
4. CTU in Prague, Faculty of Civil Engineering, Department of Architecture, Prague, Thákurova 7, Czech Republic; klara.kroftova@fsv.cvut.cz

ABSTRACT

The study of dynamic behaviour of vaults of historic buildings reveals new knowledge which can be used for the local analysis and stabilisation and rehabilitation designs of damaged vaulted structures. The analysis of the results of dynamic loading brings objective background material for the identification and localisation of failures according to MAC or COMAC criteria [1, 2] and the assessment of serviceability and structural reliability of vaulted structures of historic buildings.

KEYWORDS

Rehabilitation, Strengthening, Masonry vaults, FRP fabrics, Dynamic load, Static load

INTRODUCTION

Barrel vaults belong to the basic vaulted structures. They have been used (to a greater or lesser extent) in all architectural styles starting from Romanesque architecture and they are found in nearly every historic and heritage building. Their shape, derived from the basic cylindrical shape, is the point of departure for a whole group of vaulted structures starting from the cross vault. Barrel vaults were used for roofing buildings with square, rectangular as well as irregular plans, for roofing staircases (straight, sloping, spiral, rising) and other premises for both representative and everyday use.

At the onset of Romanesque architecture in the Czech lands, barrel vaults formed a ceiling swollen to a semi-cylindrical shape which fully sits on, “merges” with vertical masonry. In its secondary, rudimentary, purely structural function, the barrel vault survived the whole Middle Ages. Artistically treated barrel vaults can be found in single cases of two-nave and three-nave halls of townspeople’s Mazhouses in South Bohemia (Český Krumlov, Zlatá Koruna) and in gothic castles (e.g. Točnick, Švihov). From the Renaissance to the end of the 19th century, barrel vaults were commonly used for roofing both small and large spaces.

The restoration of historic buildings is frequently connected with reconstructions and rehabilitations of barrel vaults damaged mostly by the effects of induced deformations. In regions with the occurrence of natural seismicity, the failures of vaults are caused by their inelastic response to dynamic effects (Figure 1).



Fig. 1. - Vault in Loretto near Bor u Tachova

Vault failure mechanisms

The vaults failure mechanism arising by exceeding the ultimate strength (deformation) of vault masonry in tension differs from the failure mechanism of masonry pillars. The failure mechanism of vaults (curved masonry) is applied in cases where the thrust line describing the position of the origin of the internal compression force R in all vault cross sections (being the resultant curve of the loading acting on the vaults, vault supporting reactions and potential changes in vault embedding) does not pass through the inside third of the vault cross-section's height.

Vaulted structures are characterised by their high sensitivity to deformations of the supporting structure and, as a result, their response to dynamic effects causing displacements of the supporting structure (supporting system) can be the cause of an appearance of the mechanical failures or a complete failure of the vaulting system. Numerical analyses manifested high sensitivity of vaults to the deformation of the supporting structure (supports) where is, above all, the horizontal displacement (deformation) of the supports in low-order of magnitude values (mm) that can be the cause of the appearance of tensile stresses in corresponding vault sections and their successive failure due to tensile cracking. In this context, the deformations of the vault supporting structure induced by subsoil vibrations due to seismic effects may be extremely severe.

The vault failure process is very complex, including two significant mechanisms – changes in a shape, both local and of the whole vaulting system, and the vault masonry failure itself due to the action of tensile and compressive normal stresses reaching, in origins of tensile cracks where the plastic hinges appeared, ultimate values of masonry load bearing capacity in compression. The total vault failure (collapse) is, therefore, usually the result of two correlated parallel processes. It is characterised by the vault buckling together with its local failure, followed by mechanical masonry disintegration and the vault collapse. Both of the processes above are simultaneous and inseparable from each other. The vault stress state during its loading and its failure is accurately described by the thrust line pattern in individual phases of the vaulting system's action. The vault failure mechanism and reaching the vault ultimate load-bearing capacity is dramatically affected by the type of loading, particularly its potential asymmetry, its shape and geometric deflections and

imperfections and, last but not least, the stiffness and stability of the supports (Figure 2).



Fig. 2. - Vault collapse due to the supporting system's failure (horizontal displacement of supports)

The use of FRP materials in the reinforcement and stabilisation of historic, mostly masonry structures, brings numerous advantages, particularly in terms of their low weight, high effectiveness and potential reversibility [3]. The application of FRP materials in the area of historic and heritage buildings to-date has been primarily focused on the stabilisation of vertical load-bearing and vaulted structures to withstand the effects of horizontal loading induced by technical and natural seismicity [4,5].

The [NAKI I] project included extensive experimental research into the strengthening of masonry, stone, brick and mixed masonry pillars, walls and barrel vaults with composites based on high-strength, mainly carbon and glass, fibres and epoxy adhesives or polymer-modified cement mixes [7-13].

Experimental research into the response of barrel vaults to dynamic loading

Experimental research into segmented barrel vaults was performed on test pieces fabricated in a 1:1 scale – segmented masonry barrel vault sections 0.75 m in width, with a span of 3 m, with a rise of 0.75 m and a vault masonry thickness of 0.15 m, made of bricks of P15 quality and MVC 2 mortar (Table 1, Figure 3).

The objective of experimental research was the verification of the response and dynamic characteristics of segmented masonry barrel vaults exposed to repetitive static loading and dynamic loading in the horizontal and vertical direction. Nowadays, the dynamic response is very often used for the identification of potential damage to structures which need not be detectable by other means. The principle of such tests is the comparison of dynamic characteristics of structures exposed to low-level dynamic (i.e. non-destructive) excitation. The investigated characteristics are most often resonant frequencies and corresponding oscillation shapes. A change in frequency, most often its drop, may indicate the appearance of internal cracks in the tested specimen. A change in the oscillation shape, in turn, indicates its global failure.

Tab. 1. - Material characteristics of vault masonry

Vault	Mean compressive strength of bricks f_b [Mpa]	Mean compressive strength of mortar f_m [Mpa]	Mean tensile strength of mortar f [Mpa]
K 34 NZ	13.84	1.86	0.846
K 35 Z	12.18	1.16	0.586
K 36 Z	14.22	0.79	0.429

Legend:

Modulus of elasticity of bricks 2400-3600 MPa

Modulus of elasticity of mortar 400-500 MPa

Composite strips (Tyfo SCH 41 carbon fabric and Tyfo S epoxy resin) - modulus of elasticity 95800 MPa

tensile strength 986 MPa

maximum elongation 1%

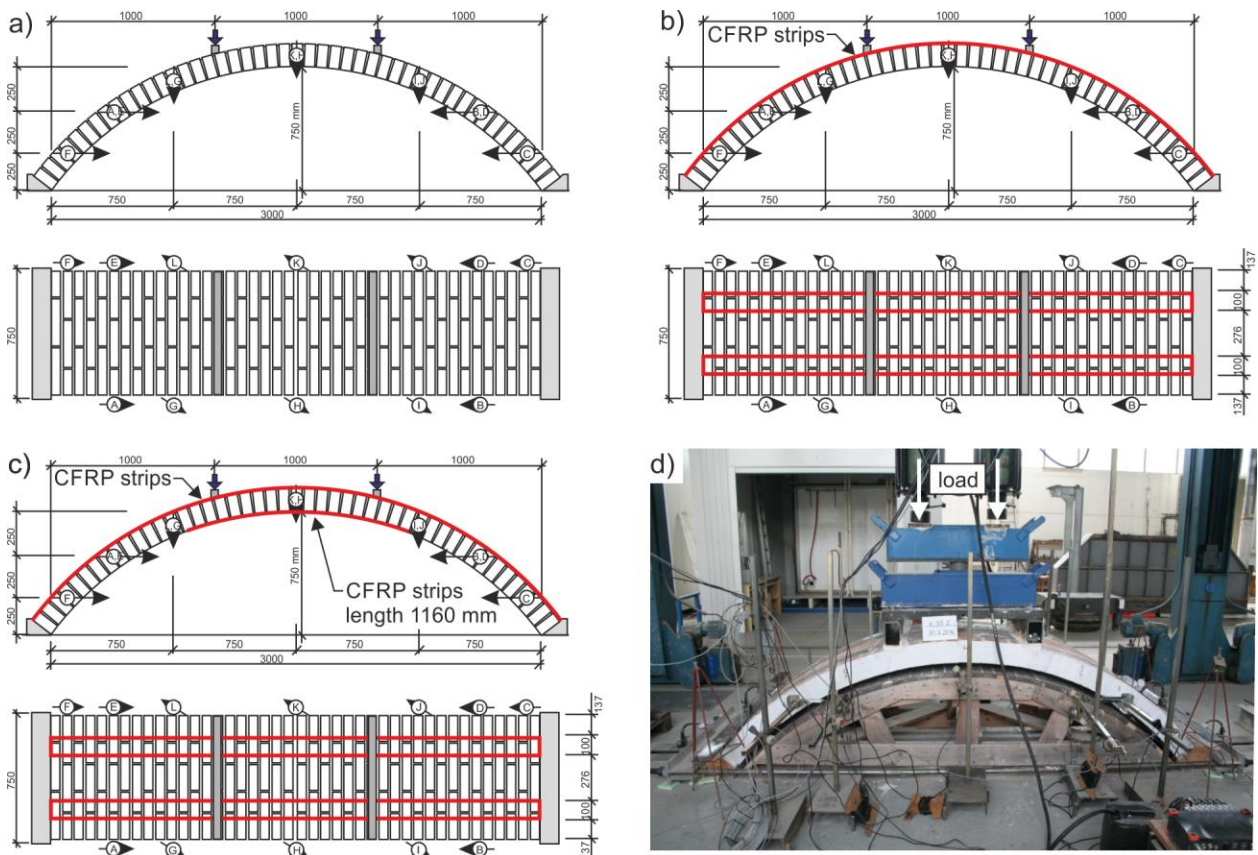


Fig. 3. - a) Scheme of vault K34 – non-reinforced, b) Scheme of vault K35 – reinforced at the extrados, c) Scheme of vault K36 – reinforced at the extrados and on the soffit, d) Test setup example

Experimental tests dealt with the verification of dynamic properties of masonry barrel vaults for the following cases:

- K34 – non-reinforced vault,
- K35 – reinforced vault, reinforcement at the extrados (upper surface) with 2 strips of the Tyfo SCH 41 carbon fabric glued with the Tyfo S epoxy resin. The strips

are 100 mm in width, the composite thickness for the calculation is 1 mm, the strips cover the whole length of the extrados. The strips (strip edges) are placed 137 mm from the vault edges.

- K36 – reinforced vault, reinforcement at the extrados (upper surface) and on the soffit (lower surface) always with 2 carbon fabric strips (see K35). The strips are 100 mm in width, the composite thickness for the calculation is 1 mm. The strips on the upper surface (extrados) again cover the whole length of the extrados, while the strips on the lower surface (soffit) are placed at the vault crown, the length of strips being 1180 mm. The strips (strip edges) are placed 137 mm from vault edges.

The experimental tests followed the procedure specified in Table 2.

Tab. 2. - Phases of dynamic and static tests of segmented barrel vaults

Phase	Tests
A – initial state	- Identification of dynamic characteristics – impact test - Performance of the static test (2x24 kN)
B – state after the first static test (2x24 kN)	- Identification of dynamic characteristics – impact test - Performance of the dynamic test in the vertical direction (Vault K34 – non-reinforced: 5Hz – 3000 oscillations; 25.96Hz – 15580 oscillations; 50Hz – 30000 oscillations, Vault K35 – reinforced at the extrados: 5Hz – 3000 oscillations; 18.44Hz – 11070 oscillations; 50Hz – 30000 oscillations, Vault K36 – reinforced at the extrados and on the soffit: 5Hz – 3000 oscillations; 19.59Hz – 6500 oscillations*)
C – state after the first dynamic loading in the vertical direction	- Identification of dynamic characteristics – impact test - Performance of the static test (2x24 kN)
D – state after the second static test (2x24 kN)	- Identification of dynamic characteristics – impact test - Performance of the dynamic test in the horizontal direction (Vault K34: 5Hz – 3000 oscillations; 20.08Hz – 12050 oscillations; 50Hz – 30000 oscillations, Vault K35 – reinforced at the extrados: 5Hz – 3000 oscillations; 24.08Hz – 14500 oscillations; 50Hz – 30000 oscillations)
E – state after the second dynamic loading in the horizontal direction	- Identification of dynamic characteristics – impact test - Performance of the static test (until failure)
F – state after the third static test (vault collapse)	

Legend: *failure of the loading device

Response of barrel vaults to static loading

The static loading of segmented barrel vaults was carried out with the help of two synchronised hydraulic actuators applying individual, monotonously rising steps of 2x 3kN. Partial results of the behaviour of barrel vaults symmetrically loaded in one third of their span with a pair of vertical forces (see Figure 3) are summarised in Table 3 and graphically displaced in Figures 4 and 5.

Tab. 3. - Experimentally identified deformation values and ultimate loading of segmented masonry barrel vaults

		K34 NZ (unreinforced)		K35 Z (CFRP, upper surface, full length)		K36 Z (CFRP, upper surface, full length, lower surface in length of 1160 mm)	
		$\delta_y^{1/2}$ [mm]	δ_x [mm]	$\delta_y^{1/2}$ [mm]	δ_x [mm]	$\delta_y^{1/2}$ [mm]	δ_x [mm]
1st static loading, load = 2 x 24 kN	$\delta_{TOT,1}$	1,43	-0,41	2,20	-0,26	1,19	0,36
	$\delta_{tot}/\delta_{TOT,1}$	100%	100%	100%	100%	100%	100%
2nd static loading, load = 2 x 24 kN	$\delta_{TOT,2}$	1,24	-0,21	1,66	-0,32		
	$\delta_{tot}/\delta_{TOT,1}$	87%	51%	75%	123%		
3rd static loading, load = 2 x 24 kN	$\delta_{TOT,3}$	1,23	-0,45	1,68	-0,21		
	$\delta_{tot}/\delta_{TOT,1}$	86%	110%	76%	81%		
3rd static loading, load-bearing capacity	$N_{u,m}$	2 x 67,7 kN (100%)		2 x 81,05 kN (120%)			
	δ_{MAX}	7,19	-3,08	16,01	-7,75		

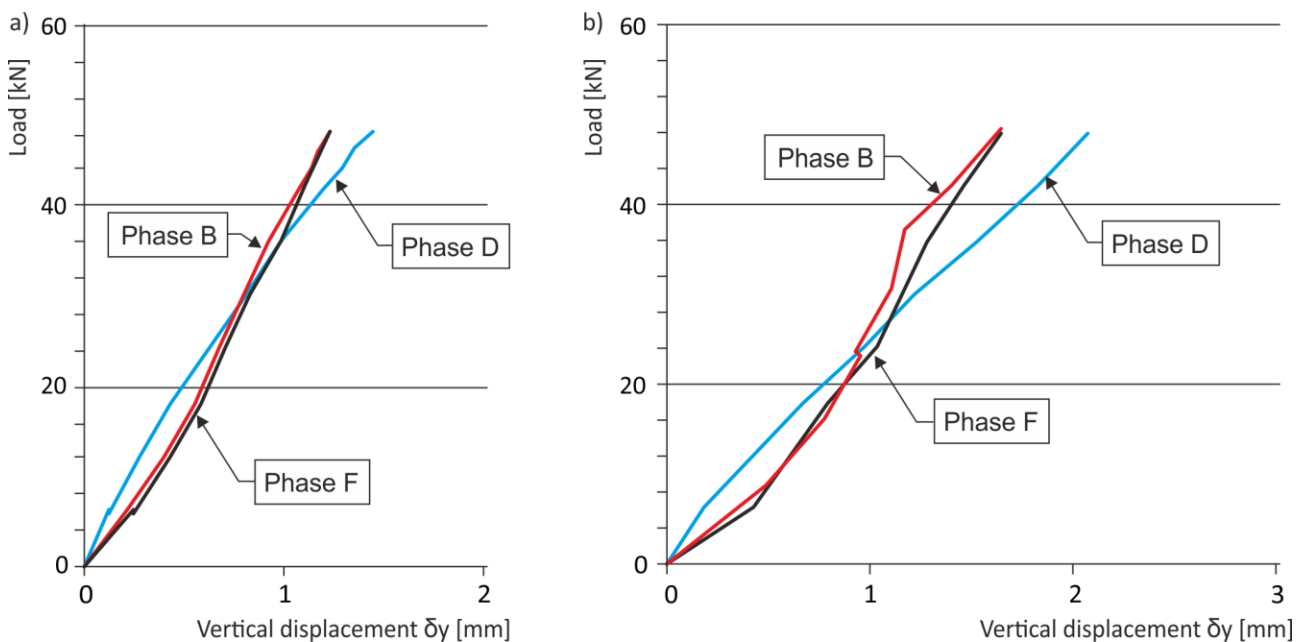


Fig. 4. - a) Pattern of vertical deformations $\delta_y \times L$ of a non-reinforced vault (K34) under static loading (2x24 kN) in individual loading phases, b) Pattern of vertical deformations $\delta_y \times L$ of a vault reinforced on the extrados (K35) under static loading (2x24 kN) in individual loading phases

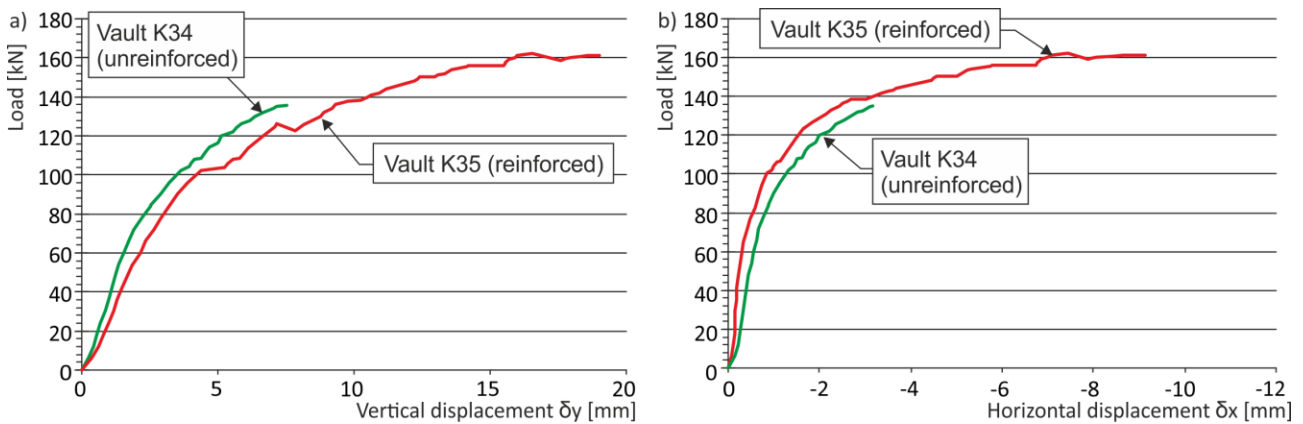


Fig. 5. - a) Overall working diagrams of vertical deformations $\delta y \times L$ of segmented barrel vaults under loading until failure, b) Overall working diagrams of horizontal deformations $\delta x \times L$ of segmented barrel vaults under loading until failure

The results of experimental values obtained from the investigation of the response of vaulted structures to static loading imply (comparison of vault deformation values from the second and third static phase – see Table 2) that the effect of dynamic loading results in the “stabilisation” (consolidation, “strengthening”) of the vaulted structure. We may presume that some portion of non-elastic deformations occurred during the first dynamic test (additional pushing of bed joints, stabilisation of the supporting system, etc.). These values can be experimentally measured (during dynamic loading) with difficulty. This issue will be the subject of further experimental verification.

Response of barrel vaults to dynamic loading

Dynamic loading in both the vertical and horizontal direction was applied with the TIRAvib electrodynamic exciter, type TV5550/LS with a weight of 550 kg. Its operating frequency range is from 0 up to 3 kHz and the maximum rated travel of mobile mass is 100 mm. The exciter was fixed to the vault and adapted to vertical and horizontal oscillations (Figure 6a). The vertical response was measured with five Wilcoxon accelerometers, model CMMS 793L, with an output sensitivity of 51 mV/ms^{-2} . One of them was positioned on the mobile part of the exciter to read the mass motion. Other sensors were positioned on the vault (Figure 6b).

Following each (partial) static loading, the vaults were exposed to dynamic loading. It was after the first static test in the vertical direction, after the second static test in the horizontal direction to verify the influence of dynamic effects on the gradual failure of a non-reinforced and reinforced vault (reduced stiffness) and to obtain findings about the effect of vault reinforcement with composites in terms of increased vault’s resistance to dynamic loading.

A total of 6 vault states were produced:

- A – initial undamaged state
- B – state after the first static test (including transition into non-linear state)
- C – state after the first dynamic loading in the vertical direction
- D – state after the second static test
- E – state after the second dynamic loading in the horizontal direction
- F – state after the third static test (until structure’s failure)

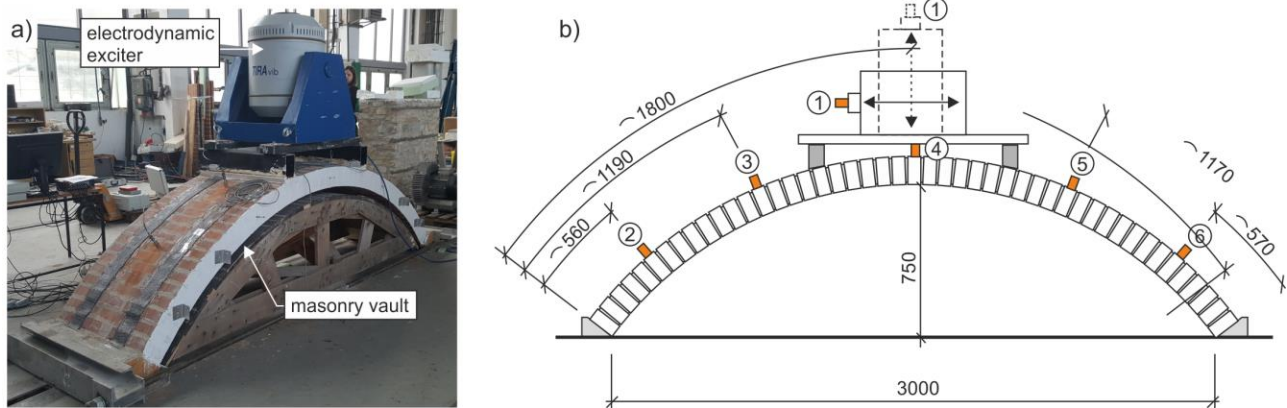


Fig. 6. - a) Mounting of the TIRAvib electrodynamic exciter on the vault, b) Distribution of sensors on the vault

Prior to each loading, the identification impact test had been performed and resonant frequencies were identified from it. The identification test had been performed with a hammer with a rubber head. The induced vault oscillations (its response) were transformed into frequency spectra from which frequency peaks were read.

Dynamic loading effects were performed both at the first resonant frequency (ca 18Hz) and outside resonant frequencies, namely at frequencies of 5Hz and 50 Hz, which characterise common external loading in buildings or traffic-induced dynamic loading.

Following each loading step, especially after static loading, there was a drop in the effective vault stiffness, which was manifested by a drop in the natural frequencies and, in some cases, by increased internal damping, most likely due to the appearance of microcracks over the whole vault cross section. Changes in stiffness and geometry after each loading step were manifested by the changes in the dynamic characteristics during the monitoring of changes in the vault's state. Frequencies were also detected on a numerical model (Figures 7 – 10) comparing theoretical and experimental oscillation shapes corresponding to the 1st to 6th natural frequencies. The obtained patterns show satisfactory agreement of theoretically and experimentally identified oscillation shapes. Successive harmonic loading occurred in the vicinity of such identified resonant frequencies with the objective of identifying also resonant oscillation shapes.

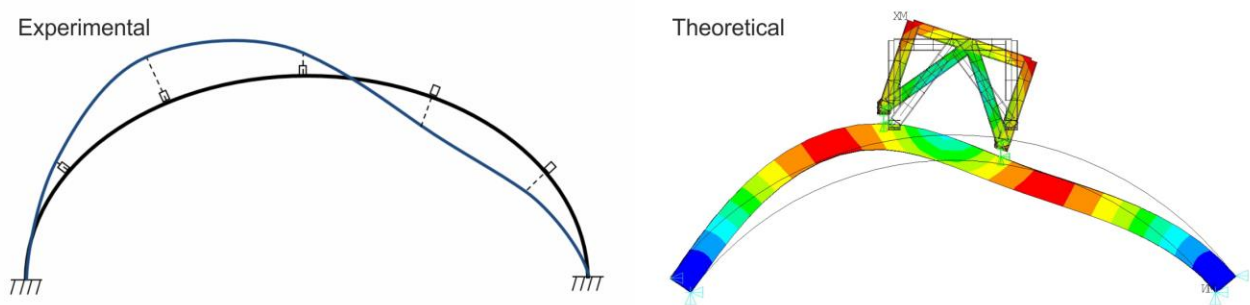


Fig. 7. - Oscillation shapes, theoretical and obtained from experiments, corresponding to the first natural frequency (see Tables 1 - 3)

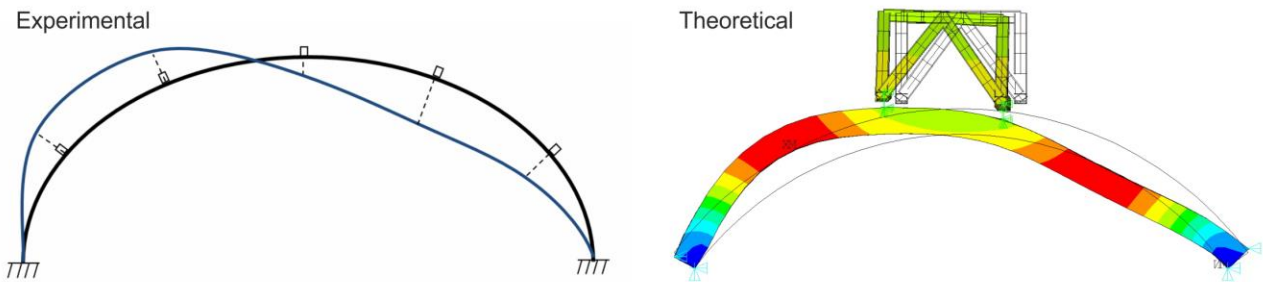


Fig. 8. - Oscillation shapes, theoretical and obtained from experiments, corresponding to the second natural frequency (see Tables 1- 3)

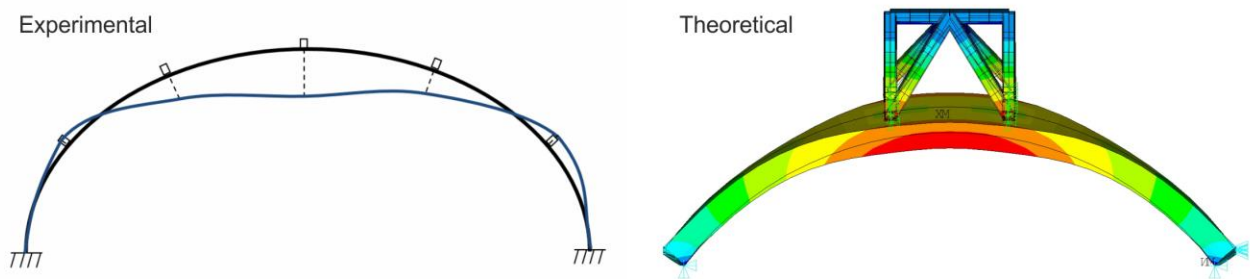


Fig. 9. - Oscillation shapes, theoretical and obtained from experiments, corresponding to the fifth natural frequency (see Tables 1 - 3)

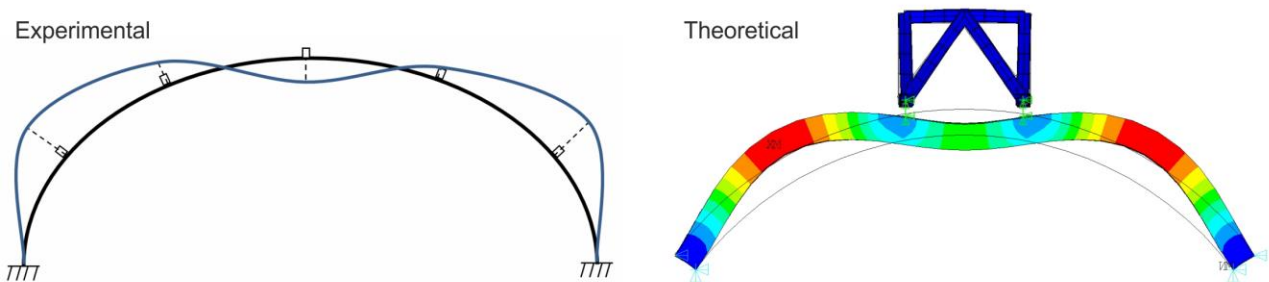


Fig. 10. - Oscillation shapes, theoretical and obtained from experiments, corresponding to the sixth natural frequency (see Tables 1 - 3)

Tables 4-6 present frequencies before loading (see Table 2) and after individual loading steps. As was assumed there is a visible drop in frequencies connected with the progressive damage of the vaulted structure. This is due to the decrease in its stiffness, which is evident mainly in non-reinforced vaulted structures. In the case of a reinforced vault, K35, there was a re-growth in frequencies detected after the second static test applying to all oscillation shapes – all frequency peaks. This is most likely caused by the cross-section's consolidation, i.e. the closing of cracks where the upper vault reinforcement probably plays a positive role. In the case of vault K34, this phenomenon is not so distinctive, the frequencies only rise in the first resonant shape, which is dominant, i.e. very important for the detection of damage.

Tab. 4. - Selected frequencies measured after different types of loading for vault K34_NZ

Loading	Frequencies [Hz]								
	1	2	3	4	5	6	7	8	9
Before loading	17.55	28.26	32.20	50.66	65.61	69.27	82.70	105.1	113.2
After 1 st static test	17.85	27.62	31.89	50.05	62.1	65.16	--	98.42	106.7
After 1 st static test + 1 st dyn. loading	13.58	27.62	32.2	--	--	--	--	93.99	--
After 2 nd static test	14.04	24.72	28.69	43.03	59.81	--	--	93.99	107.4
After 2 nd stat. test + 2 nd dyn. loading	14.04	24.72	28.69	41.45	--	66.53	73.85	92.47	107.1

Tab. 5. - Selected frequencies measured after different types of loading for vault K35_Z

Loading	Frequencies [Hz]								
	1	2	3	4	5	6	7	8	9
Before loading	19.23	29.75	33.26	47.76	56.3	66.53	72.63	105.1	110.3
After 1 st static test	14.42	23.19	29.68	41.35	50.58	63.4	72.25	103.8	107.0
After 1 st static test + 1 st dyn. loading	13.43	19.53	28.53	36.01	49.59	62.87	69.58	97.05	--
After 2 nd static test	15.87	24.72	29.91	--	50.96	62.87	74.16	97.6	103.8
After 2 nd stat. test + 2 nd dyn. loading	13.28	22.28	28.08	--	48.68	62.56	74.92	89.42	103.3

Tab. 6. - Selected frequencies measured after different types of loading for vault K36_Z

Loading	Frequencies [Hz]								
	1	2	3	4	5	6	7	8	9
Before loading	19.99	32.04	34.71	51.19	64.47	86.98	100.0	105.6	110.8
After 1 st static test	--	24.41	31.89	49.9	--	69.27	96.74	102.2	105.1

Legend: The test was interrupted for the reason of the electrodynamic exciter's failure.

CONCLUSION

Experimental results represent very important background material for numerical modelling during a repetitive validation of the computational model, but also a significant source of information for the selection of effective rehabilitation procedures for vaulted structures. The results are of major importance particularly for vaults of historic buildings situated in the seismically active



regions or in places with intensive technical and induced seismicity (mining, stone quarrying, traffic).

ACKNOWLEDGEMENTS

The article was written with support from the NAKI II DG16P02M055 project "Research and development of materials, processes and techniques for restoration, preservation and strengthening of historic masonry structures, surfaces and systems for preventive care of heritage buildings exposed to anthropogenic and natural risks" of the Ministry of Culture of the Czech Republic.

REFERENCES

- [1] M. Pimer, S. Urushadze. " Structural damage assessment using dynamic response, Acta technica , CSAV 47, 2002, pp. 445-466.
- [2] M. Pimer, S. Urushadze: Dynamic response as a tool for damage identification, Applied Mechanics, International research Journal, Timoshenko Institute of Mechanics, Kiev, Ukraine, ISSN 0032-8243, App. Mech., 2004, Vol. 40, N 5, 1-144, Editor: A.N. Guz, pp.3-29.
- [3] Bruggi, M., Milani, G., Taliercio, A., Design of the Optimal Fiber-Reinforcement for Masonry Structures via Topology Optimization, International Journal of Solids and Structures 2013, doi: <http://dx.doi.org/10.1016/j.ijsolstr.2013.03.007>
- [4] Luccioni B, Rougier VC, In-plane retrofitting of masonry panels with fibre reinforced composite materials, Construction and Building Materials 2011;25:1772–1788
- [5] Grande E, Imbimbo M, Sacco E, Finite element analysis of masonry panels strengthened with FRPs, Composites: Part B 2013;45:1296–1309
- [6] Výzkumný projekt Ministerstva kultury ČR NAKI DF12P01OVV037 "Progresivní neinvazivní metody stabilizace, konzervace a zpevnování historických konstrukcí a jejich částí kompozitními materiály na bázi vláken a nanovláken", vedoucí řešitel prof. Ing. Jiří Witzany, DrSc. dr.h.c.
- [7] Witzany, J., Zigler, R., Kroftová, K. Strengthening of compressed brick masonry walls with carbon composites (2016) Construction and Building Materials, 112, pp. 1066-1079. DOI: 10.1016/j.conbuildmat.2016.03.026
- [8] Witzany, J., Zigler, R. Stress state analysis and failure mechanisms of masonry columns reinforced with FRP under concentric compressive load (2016) Polymers, 8 (5), art. no. 176, . DOI: 10.3390/polym8050176
- [9] Witzany, J., Zigler, R. Failure mechanism of compressed reinforced and non-reinforced stone columns (2015) Materials and Structures/Materiaux et Constructions, 48 (5), pp. 1603-1613. DOI: 10.1617/s11527-014-0257-z
- [10] Witzany, J., Brožovský, J., Čejka, T., Kroftová, K., Kubát, J., Makovička, D., Zigler, R. The application of carbon composites in the rehabilitation of historic baroque vaults (2015) Polymers, 7 (12), pp. 2670-2689. DOI: 10.3390/polym7121540
- [11] Witzany, J., Čejka, T., Zigler, R. Failure mechanism of compressed short brick masonry columns

confined with FRP strips, (2014) *Construction and Building Materials*, 63, pp. 180-188.
DOI: 10.1016/j.conbuildmat.2014.04.041

[12] Witzany, J., Zigler, R. The analysis of the effect of strengthening compressed masonry columns with carbon fabric (2014) *Proceedings of the 7th International Conference on FRP Composites in Civil Engineering, CICE 2014*.

[13] Witzany, J. - Čejka, T. - Zigler, R.: Experimental research on strengthening of masonry vaults using FRP. In *FRP Composites in Civil Engineering*. Duebendorf, Švýcarsko: EMPA, 2008, p. 149. ISBN 978-3-905594-50-8.